THE JOURNAL OF PHYSICAL CHEMISTRY B

Article

pubs.acs.org/JPCB

Time-Resolved Spectroscopy of Ultrafast Photoisomerization of Octopus Rhodopsin under Photoexcitation

Atsushi Yabushita,*[,†] Takayoshi Kobayashi,[†,‡,§,∥] and Motoyuki Tsuda[⊥]

[†]Department of Electrophysics, National Chiao-Tung University, Hsinchu 300, Taiwan

[‡]CREST, Japan Science and Technology Agency, 4-1-8, Honcho, Kawaguchi, Saitama 332-0012, Japan

[§]Department of Applied Physics and Chemistry and Institute for Laser Science, University of Electro-Communications, 1-5-1, Chofugaoka, Chofu, Tokyo 182-8585, Japan

[∥]Institute of Laser Engineering, Osaka University, 2-6 Yamada-oka, Suita, Osaka 565-0971, Japan

[⊥]Kagawa School of Pharmaceutical Sciences, Tokushima Bunri University, 1314-1 Shido, Sanuki, Kagawa 769-2193, Japan

ABSTRACT: A primary process in vision is the *cis*−*trans* photoisomerization of a chromophore of rhodopsin, called retinal. In the present work, we have performed ultrafast time-resolved spectroscopy of octopus rhodopsin using a sub-5-fs pulse laser. In comparison with our previous study on bacteriorhodopsin, we found that octopus rhodopsin follows similar dynamics after photoexcitation but with different time constants. Spectrogram analysis showed that a C═N stretching mode appeared directly after photoexcitation. After reaching the conical intersection region at 80 fs, the overlapping hydrogen out-of-plane and in-plane C═C−H modes emerged as distinct peaks at ∼200 fs, finishing a rapid relaxation along the coordinate related with these modes. The intensities of these peaks and a C═C stretching mode were found to be modulated at a period of ∼500 fs, reflecting torsional motion around the C═C double bond before thermalization with the distribution of structural variations in the all-*trans* structure in configuration space.

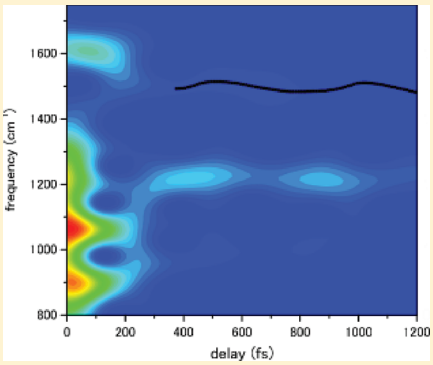

1. INTRODUCTION

The visual process in a photoactive cell consists of a series of chemical reactions mediated via several intermediates and culminating in stimulation of the optic nerve. Rhodopsin (Rh) is a photoreceptive pigment for twilight vision, which consists of the apoprotein opsin and the 11-*cis*-retinal chromophore. Photoexcitation of Rh leads to a series of intermediates that eventually initiate an enzyme cascade triggering electric excitation.[1−5]The Rh pigment has been studied more than any other visual pigment, including those responsible for color vision, because of its relatively easy preparation. The following section describes the current understanding of the photoisomerization of retinal based on previous studies.[6−27]

The first intermediate of Rh is called primeRh[8] (or photoRh[9]) and the second intermediate, identified earlier than the first, is called bathoRh.[2] Comparison of the absorption spectrum of primeRh[10] and studies of 11-*cis*-locked Rh[11,12] indicated that the chromophore in primeRh has a distorted all-*trans* configuration. Therefore, to form bathoRh, the chromophore must undergo *cis*−*trans* isomerization. Studies on the *cis*−*trans* isomerization yield of the Rh chromophore in solution[13,14] and in protein[15] have shown that the isomerization yield is enhanced by more than an order of magnitude in the protein environment. Other studies have inferred that the first intermediate (primeRh) is the nonthermal state of bathoRh.[16,17] The transitions between the intermediates and their time constants have been reported as follows. After photoexcitation of Rh, a Franck−Condon (FC) state proceeds to a conical intersection (CI) on the potential energy surface of the electronic excited state in ∼100 fs as estimated in time-resolved measurements.[6,17−20] Femtosecond transient absorption measurement has elucidated that curve crossing to the ground state takes about 200 fs to form the highly distorted primeRh.[21] Picosecond Raman study clarified that a temporal decay of a few picoseconds corresponds to conversion from primeRh to bathoRh.[22]

Relatively few studies[18−21] exist on the ultrafast dynamics of Rh because of the difficulties in preparation due to the fragility of the samples. In place of detailed studies on Rh, bacteriorhodopsin (bR) has been extensively studied as a model system as it is relatively robust in experiments. In the femtosecond time-resovled stimulated Raman study of bR,[23] the photoisomerization of bR has been reported to follow the process

$$\mathrm{bR} \xrightarrow{h\nu} \mathrm{FC(H)} \xrightarrow{<200\ \mathrm{fs}} \mathrm{CI(I_{460})} \xrightarrow{500\ \mathrm{fs}} \mathrm{J} \xrightarrow{3\ \mathrm{ps}} \mathrm{K} \rightarrow \cdots$$

In a previous work we performed ultrafast time-resolved spectroscopy of bR to clarify its electronic dynamics and

Received: September 28, 2011
Revised: December 17, 2011
Published: January 17, 2012

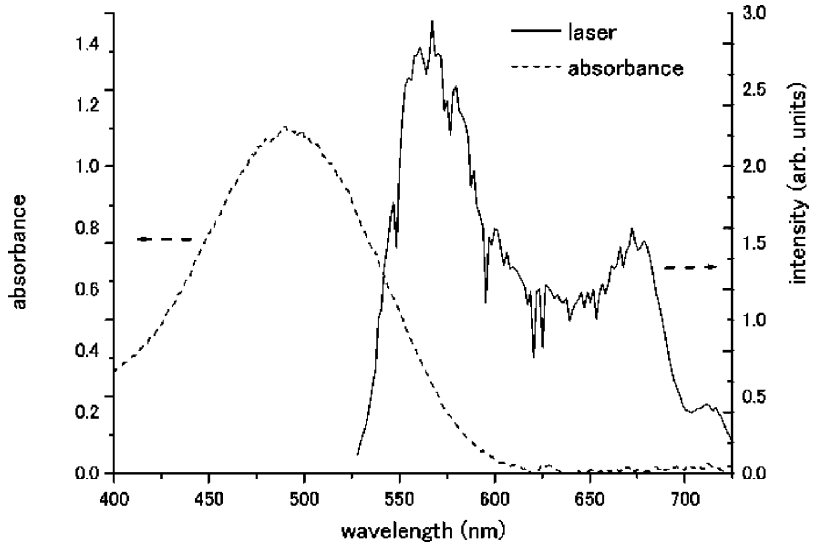

Figure 1. Laser spectrum (solid line) and absorption spectrum (dotted line) of octopus Rh.

vibration dynamics in detail.[24] The results elucidated the dynamics of the intermediates, which have lifetimes consistent with previous reports on dynamic hole-burning,[25] time-resolved fluorescence,[26] and transient absorption.[27] However, the relaxation dynamics of bR and Rh are expected to be quite different considering the differences in structural transition between the retinal in bR (from all-*trans* to 13-*cis* configuration) and that in Rh (from 11-*cis* to all-*trans* configuration).

In the present work, we have performed ultrafast time-resolved spectroscopy of octopus Rh using a sub-5-fs laser pulse and a 128-channel detection system. The ultrafast time resolution of sub-5-fs enabled us to study both the electronic and vibration dynamics, and the multichannel detector array allowed simultaneous observation of the signals over all probe wavelengths, avoiding sample degradation. The observed ultrafast dynamics of Rh showed a difference from the results for bR obtained in the previous work, as the present work clarified that the transition from the FC state to CI proceeds faster in octopus Rh than in bR.

2. EXPERIMENTAL METHODS

Femtosecond Spectroscopy Apparatus. The pulsed-light sources and setup for femtosecond time-resolved absorption spectroscopy used in this work are described in previous reports from our group.[28−30] A 4.7-fs, 1-kHz pulse train was generated from a noncollinear optical parametric amplifier (NOPA) with a pulse compressor,[28] covering a wavelength range from 528 to 727 nm. The laser spectrum obtained by NOPA is shown in Figure 1. The energy and peak intensity of the pump pulses at the sample were ∼10 nJ and 10 GW/cm^2, respectively, which are approximately 10 times higher than the probe pulses. The pulse energies (intensities) of the pump and probe pulses at the sample position were approximately 20 and 5 nJ (7.5×10^{14} and 8.5×10^{13} photons/cm^2), respectively.

In order to measure weak pump−probe signals at various wavelengths, we used a multichannel lock-in amplifier, which was specifically designed for the simultaneous detection of low-intensity signals over the entire spectral region. The multichannel lock-in amplifier consists of 128 lock-in amplifiers connected to 128 avalanche photodiodes. In the present experiment, multichannel signals, spectrally resolved by a polychromator (JASCO M25-TP), were detected by the avalanche photodiodes with the lock-in amplifiers in reference to pump pulses modulated at 500 Hz by a mechanical chopper. The normalized transmittance changes in the range extending from 528 to 727 nm were measured for −100 to 2000 fs with a 1-fs interval.

Octopus Rh. The microvillar membranes of the octopus retina (Mizudako, *Paroctopus dofleini*) were isolated by sucrose flotation (34 wt %, buffer A) (400 mM KLC, 10 mM $MgCl_2$ + 20 μM p-APMSF) repeated twice. The obtained pellet was washed several times with buffer A and with buffer B (10 mM MOPS [pH 7.4], 1 mM DTT, 20 μM p-APMSF). The final products were suspended in buffer B and kept at −80 °C in the dark. A part of this frozen sample was thawed and centrifuged. The as-obtained pellet was solubilized in H_2O with 2 mM MOPS [pH 7.4] and 2% sucrose monolaurate (L-1690 or SM-1200). The solution was centrifuged, and the supernatant was used as the sample, which was added to a 1 mm-thick stationary optical cell for experiments without circulation. The absorption spectrum of the sample showed no difference between before and after the pump−probe measurement within the margin of the error of about 10%. The peak absorbance at 490 nm of the sample solution was 1.1. The absorption spectrum of the octopus Rh is plotted in Figure 1 together with the laser spectrum.

3. RESULTS AND DISCUSSION

Figure 2a shows the real-time absorption difference spectra, ΔA, in the time region between −100 and 2000 fs over the spectral region from 528 to 727 nm. Real-time traces probed at 577, 610, 641, and 682 nm are shown in Figure 2b. In all the observed spectral regions, the sign of ΔA was positive in the initial period following photoexcitation, which is thought to reflect induced absorption. Relaxation from the FC state (named the H state in the case of bR) in the first electronic excited state to a geometrically relaxed state such as a twisted state, which is called the I state in the case of bR, is associated with the decrease in the positive ΔA signal. This is induced by

dx.doi.org/10.1021/jp209356s | J. Phys. Chem. B 2012, 116, 1920−1926

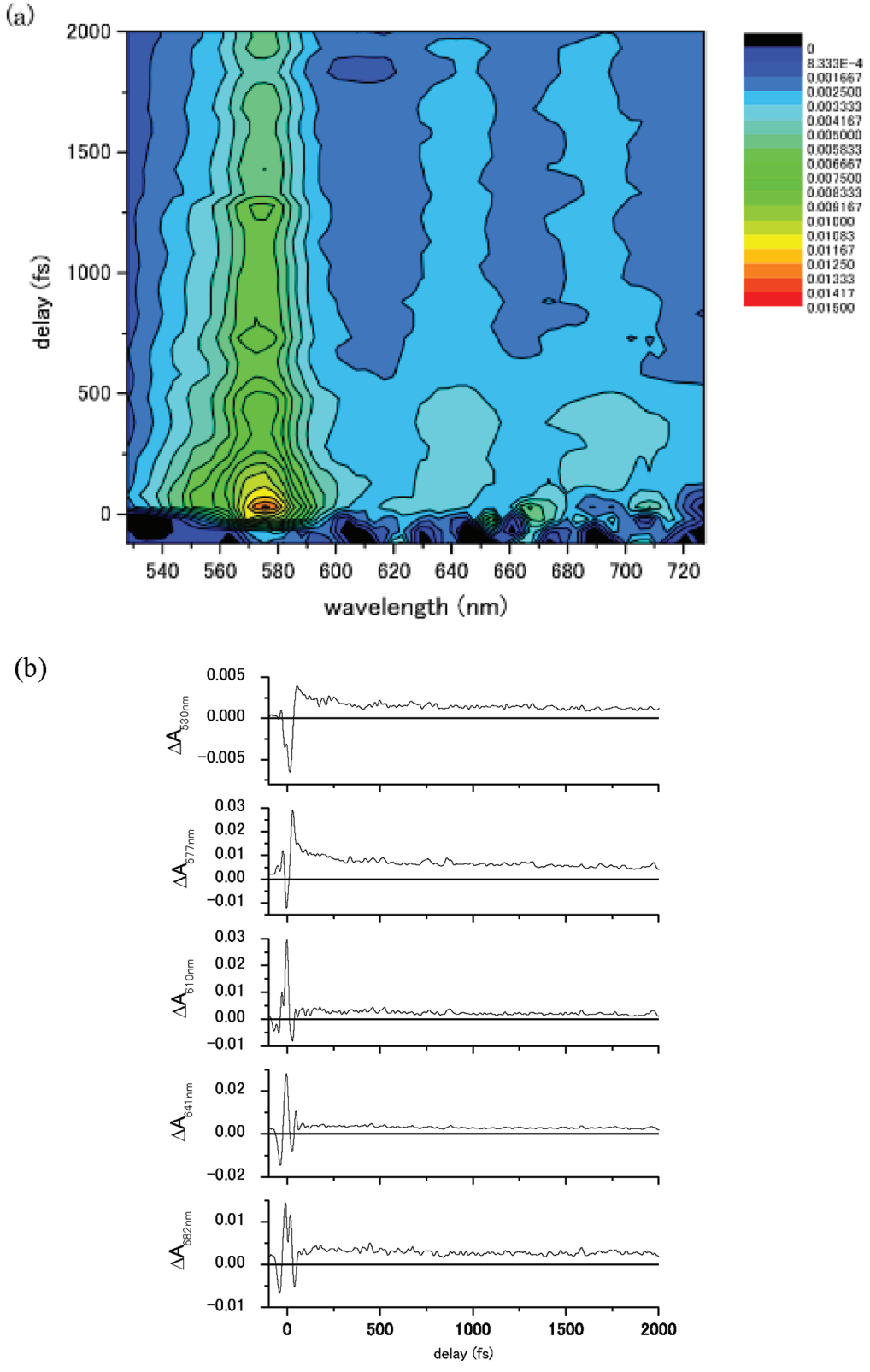

Figure 2. Observed time-resolved difference absorption spectra. (a) Two-dimensional display of measured time-resolved difference absorption spectra $\Delta A(t,\lambda)$. (b) Real-time traces of the absorbance difference for five probe wavelengths.

the spectral blue shit of the induced absorption. The shift takes place because the induced absorption is affected by the energy stabilization and destabilization of the initial state (I state in the case of bR) and the final state (FC state of the induced absorption from the I state), respectively. The oscillatory features around time zero are considered to be coherent artifacts generated by the interference between probe light and scattered pump light.

dx.doi.org/10.1021/jp209356s | J. Phys. Chem. B 2012, 116, 1920−1926

The photoexcited Rh is reported to decay by the following process:[6,7,20]

$$\mathrm{Rh} \xrightarrow{h\nu} \mathrm{FC} \xrightarrow{<100\ \mathrm{fs}} \mathrm{CI} \xrightarrow{100-300\ \mathrm{fs}} \mathrm{primeRh} \xrightarrow{1-4\ \mathrm{ps}} \mathrm{bathoRh} \xrightarrow{>1\ \mathrm{ns}} \quad (1)$$

where FC indicates the Franck−Condon state. The FC and CI were previously called the H state and J state, respectively, as described above.

Electronic Dynamics. To determine the lifetimes and spectra of the decaying components, we fitted the observed time-resolved difference absorption spectra $\Delta A(t,\lambda)$ using a global fitting method[31] over all probe wavelengths. The fitting function included three components as follows, representing two transitions with distinct time constants:

$$\Delta A(t,\lambda) = \Delta A_0(\lambda) + \Delta A_1(\lambda)\exp(-t/\tau_1) + \Delta A_2(\lambda)\exp(-t/\tau_2) \quad (\tau_1 < \tau_2) \quad (2)$$

Finding the condition for least-squares error in the global fit analysis, we have estimated the time constants of τ_1 and τ_2 as 80 fs and 1.1 ps, respectively. The two time constants reflect the sequential relaxation after photoexcitation. The whole process can be expressed by

$$\Delta A(t,\lambda) = \Delta A_a(\lambda)\exp(-t/\tau_1) + \Delta A_b(\lambda) \times [1-\exp(-t/\tau_1)]\exp(-t/\tau_2) + \Delta A_c(\lambda)[1-\exp(-t/\tau_1)] \times [1-\exp(-t/\tau_2)] \quad (3)$$

where $\Delta A_i(\lambda)$ (i = a, b, c) is the spectrum of each intermediate. Considering $\tau_1 \ll \tau_2$, eq 3 can be approximated as

$$\Delta A(t,\lambda) = \Delta A_a(\lambda)\exp(-t/\tau_1) + \Delta A_b(\lambda) \times [\exp(-t/\tau_2) - \exp(-t/\tau_1)] + \Delta A_c(\lambda)[1-\exp(-t/\tau_2)] \quad (4)$$

Using eqs 2 and 4, we obtain

$$\Delta A_1(\lambda) = \Delta A_a(\lambda) - \Delta A_b(\lambda) \quad (5)$$

$$\Delta A_2(\lambda) = \Delta A_b(\lambda) - \Delta A_c(\lambda) \quad (6)$$

$$\Delta A_0(\lambda) = \Delta A_c(\lambda) \quad (7)$$

Equations 5-7 give

$$\Delta A_a(\lambda) = \Delta A_0(\lambda) + \Delta A_1(\lambda) + \Delta A_2(\lambda) \quad (8)$$

$$\Delta A_b(\lambda) = \Delta A_0(\lambda) + \Delta A_2(\lambda) \quad (9)$$

Spectra of $\Delta A_0(\lambda)$, $\Delta A_1(\lambda)$, and $\Delta A_2(\lambda)$ were estimated by least-squares fit of $\Delta A(t,\lambda)$ using the two obtained time constants of τ_1 and τ_2. Using eqs 7−9, $\Delta A_a(\lambda)$, $\Delta A_b(\lambda)$, and $\Delta A_c(\lambda)$ were calculated from the spectra of $\Delta A_0(\lambda)$, $\Delta A_1(\lambda)$, and $\Delta A_2(\lambda)$, and the result is plotted in Figure 3a. The three spectra were normalized for their comparison in Figure 3b.

Previous work by Shank and Mathies and others observed the signal rise on a 100 fs time scale in their study of femtosecond transient absorption measured by 35-fs pump pulses, and concluded that the wavepacket rapidly leaves the FC region in the 100 fs time scale.[32] Mathies claimed to have found that the system is carried toward CI in ~50 fs in his study of femtosecond stimulated Raman spectroscopy using 30-fs photochemical pump pulses.[7] It implies that τ_1 (80 fs) obtained in the present work corresponds to the time moving from the FC region to CI. In the present work, we could determine the time constant using a much shorter pulse of sub-5-fs pulses. The spectrum of $\Delta A_a(\lambda)$ in eq 3 has a negative value, which is thought to reflect the induced absorption of the FC state.

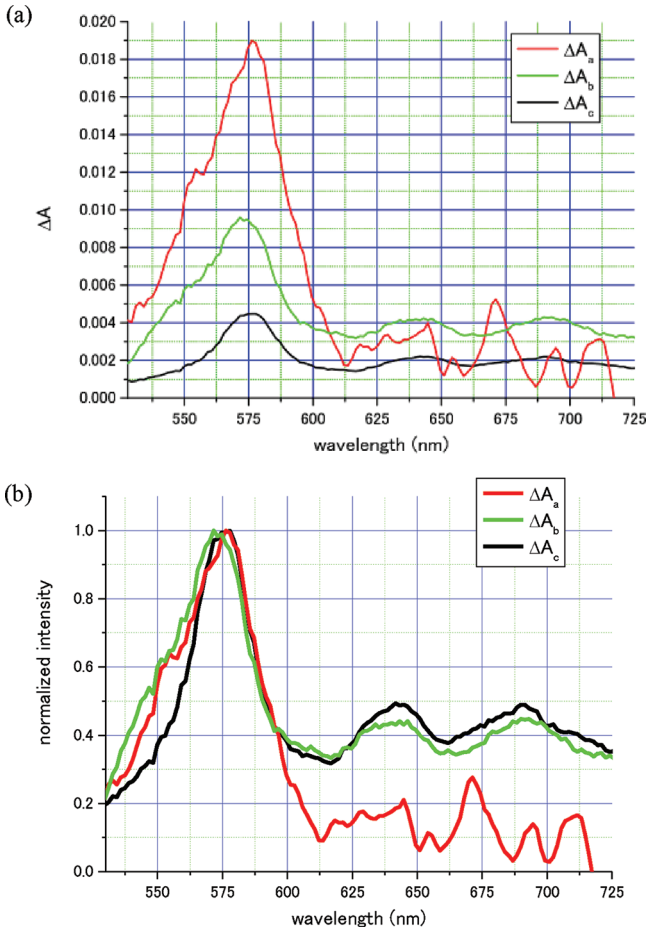

Figure 3. Results of global fitting analysis. (a) Mean square error calculated scanning the value of τ_1 and τ_2. (b) Spectra of $\Delta A_a(\lambda)$, $\Delta A_b(\lambda)$, and $\Delta A_c(\lambda)$ calculated from the spectra of $\Delta A_i(\lambda)$ (i = 0,1,2). The spectra of $\Delta A_i(\lambda)$ were obtained in least-squares fit of $\Delta A(t,\lambda)$ using τ_1 and τ_2 estimated in panel a.

Spectra of $\Delta A_b(\lambda)$ and $\Delta A_c(\lambda)$ show similar spectral shape with positive value in the all-probe wavelength region, reflecting induced absorption of reaction intermediates. The spectrum of $\Delta A_c(\lambda)$ around 575 nm is narrower than the spectrum of $\Delta A_b(\lambda)$. The narrowing of the spectrum is considered to be caused by the vibration cooling on the ground state potential surface. Therefore $\Delta A_b(\lambda)$ and $\Delta A_c(\lambda)$ are thought to correspond to the induced absorption of primeRh and bathoRh, respectively. This implies that primeRh becomes thermalized into bathoRh in the time constant of τ_2.

Vibration Dynamics. Wavepacket motion in the electronic excited state and that in the electronic ground state modulate the $\Delta A(t)$ traces. Therefore, Fourier analysis of the $\Delta A(t)$ traces reflects the vibrational modes either of the photoactive state or the nonphotoactive state. The vibration mode signals of the nonphotoactive state are expected to decay without

dx.doi.org/10.1021/jp209356s | J. Phys. Chem. B 2012, 116, 1920−1926

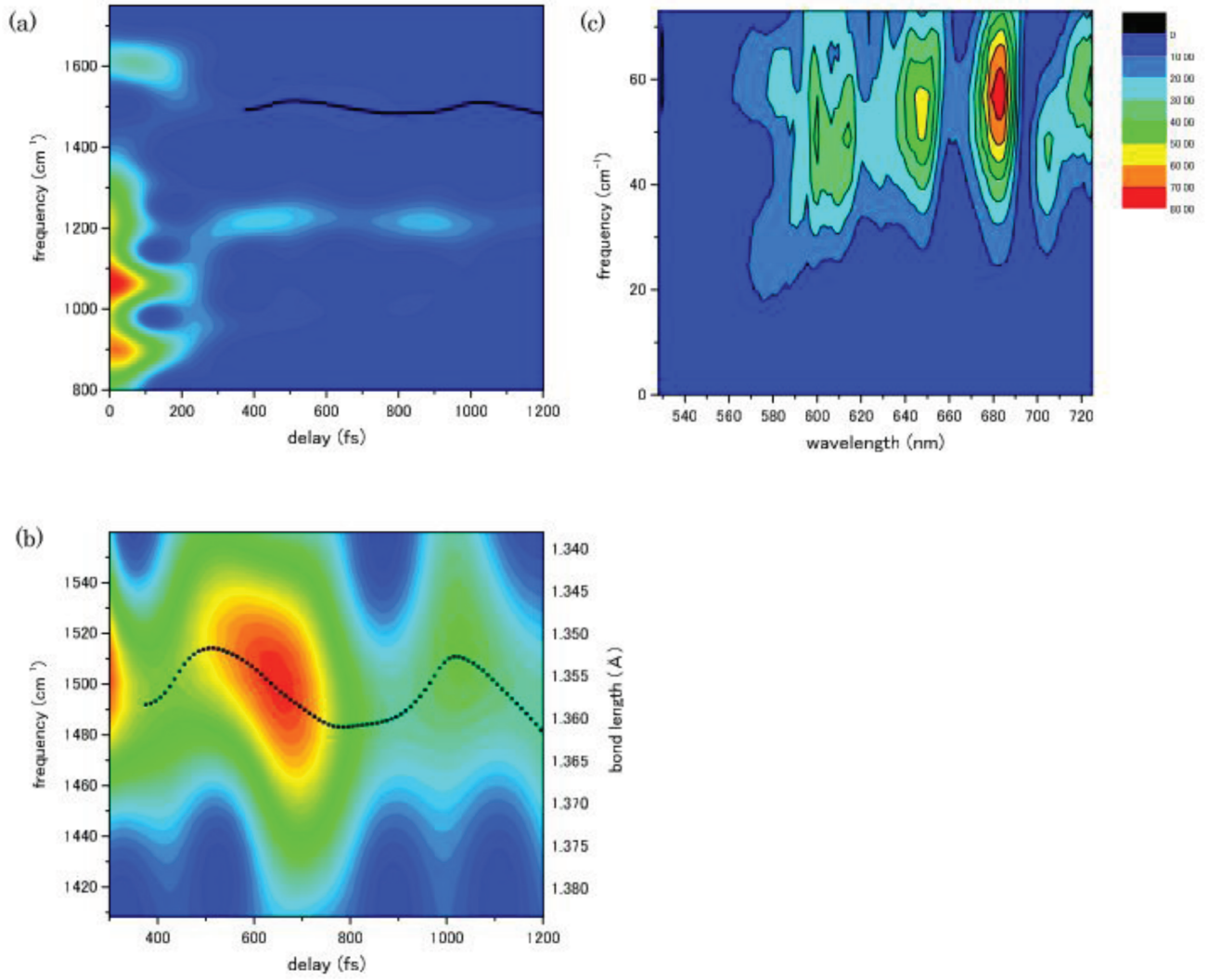

Figure 4. Spectrograms calculated from the ΔA traces at 530 nm. The black dots show the C═C stretching mode. Spectrograms are shown for the (a) 900−1750 cm^{-1} range and (b) the 1410−1560 cm^{-1} range rescaled in intensity to show the frequency modulation of the C═C stretching mode. (c) Two-dimensional Fourier power spectra of the time-resolved difference absorption traces $\Delta A(t)$ over delay times ranging from 800 to 2000 fs.

frequency shift or modulation. Therefore, the vibration mode signals showing frequency shift or modulation are thought to be assigned to the dynacmics of the vibration mode coupled to the photoactive state. In the following, we discuss the vibration mode signals showing frequency shift or modulation to discuss the dynamics of the vibration mode coupled to the photoactive state

Fourier power spectra of the time traces of the absorption difference exhibit three prominent modes at around 1550, 1200, and 1000 cm^{-1} assigned to C═C stretching ($\nu_{C=C}$), C−C stretching (ν_{C-C}), and hydrogen out-of-plane (HOOP) modes, respectively. The dynamics of those vibration modes at each probe wavelength can be studied by calculating the instantaneous molecular vibration frequencies using spectrogram analysis[33,34] of the time-resolved difference absorption traces. A Blackman window with a fwhm of 240 fs was used as a gate function in the spectrogram calculation. Figure 4a shows the calculated spectrograms at a probe wavelength of 530 nm. For delay times shorter than 150 fs, the spectrogram shows the existence of a C═N stretching mode at a frequency of ∼1610 cm^{-1}, which quickly decays in a similar fashion to that observed in photoisomerization of bR.[24] This confirms that the primary event after photoexcitation of the octopus Rh is a deformation of the retinal configuration near the C═N bond of the protonated Schiff base.

Just after the photoexcitation, strain in retinal is localized around the Schiff base and propagates to surrounding C═C bonds within a few hundred femtoseconds. Therefore the C═N stretching mode is more distinct than the C═C stretching mode in the early time scale. The reason why the observed frequency of the C═N stretching mode (1610 cm^{-1}) was lower than that of the ground state reported as ∼1650 cm^{-1} in Raman study[35] can be explained as follows in the analogy of the explanation for bR.[36] The Schiff base forms a hydrogen bond to its salt bridge partner in the ground state. The primary process after photoexcitation involves a movement of the Schiff base proton away from a counterion, which breaks the hydrogen bond and causes a red-shift of the C═N stretching frequency.

Figure 4b shows a spectrogram of the 1410−1560 cm^{-1} range with rescaled intensity to clearly show the frequency modulation in the C═C stretching mode. The spectrogram is a time-frequency analysis using the sliding Fourier transform window and an artifact can appear in the spectrogram trace as a modulation of frequency and intensity that is caused by a beat

dx.doi.org/10.1021/jp209356s | J. Phys. Chem. B 2012, 116, 1920−1926

between neighboring frequency modes.[37] The modulation period corresponds to the inverse of the frequency difference between the neighboring modes. When the time width of the sliding window is much shorter than the modulation period of the artifact, the spectrogram trace is significantly contaminated by the artifact. The observed frequency modulation in Figure 4b has a period of 500 fs, which corresponds to 67 cm^{-1}. If the frequency modulation is caused by an artifact, neighboring frequency modes separated by 67 cm^{-1} should be observed in the Fourier power spectrum of the time-resolved difference absorption trace. However, the Fourier power spectrum calculated from the time-resolved trace in the region from 200 to 1200 fs did not show a neighboring mode around 1500 cm^{-1} separated by 67 cm^{-1}. It confirms that the frequency modulation observed in the spectrogram trace is not an artifact caused by the beat between neighboring modes, but reflects a real-time frequency change of the vibration frequency.

After photoisomerization of the retinal is completed, the frequency of the C=C stretching mode was found to be modulated at a period of ~500 fs. The frequency modulation reflects the wavepacket motion on the potential energy surface of the relevant electronic states of all of the ground state, the excited state, prime Rh, and bathoRh, which appear after the photoexcitation.[38,39] This value for octopus Rh is consistent with the period of 550 fs observed in the wavepacket motion results on bovine Rh reported by Shank et al.,[40] and is considerably different from the period of ~200 fs in bR.[27] The frequency modulation reflects torsional motion around the C_{11}=C_{12} double bond before thermalization in the all-*trans* structure. The change in the frequency can be ascribed to modulation of the bond length of the C_{11}=C_{12} double bond using an empirical equation relating the bond length and vibration frequency. The empirical equation is obtained as follows.

The relationship between the bond-stretching force constant k (dyn/cm), bond length d (Å), π bond order (P), and electronegativity (χ) was found by Gordy as follows:[41]

$$k = a(P + 1)\left(\frac{\chi}{d}\right)^{3/2} + b \tag{10}$$

Here, a and b are empirical constants equal to 1.67×10^5 and 0.30×10^5, respectively, for stable molecules exhibiting their normal covalencies. Gordy has estimated the average deviation of k calculated from k values observed for 71 cases to be 1.84%. The bond vibration frequency ν (cm^{-1}) can then be related to the bond-stretching force constant k (dyn/cm) assuming an isolated oscillator as

$$\nu = \left(\frac{1}{2\pi^2 c^2 m}\right)^{1/2} k^{1/2} \tag{11}$$

where m and c are the mass of the bonded atom and the velocity of light, respectively.[42] Taking eqs 1 and 2, we can obtain the relation between the bond length d and the vibration frequency ν as

$$\nu = C\left[a(P + 1)\left(\frac{x}{d}\right)^{3/2} + b\right]^{1/2} \tag{12}$$

where χ = 2.5 and C = 1.66. Dewar derived the relationship between the bond length d and the bond order P for single and double bonds as d = 1.489−0.151P.[43] For a single bond, P is 0, and for a double bond, P is 1. Using this equation, the observed frequency change in the C=C stretching mode leads to a modulation in the bond length of the C_{11}=C_{12} double bond of ~11 ± 2 mÅ.

The assignment was certified by the direct observation of the real-time frequency of the HOOP mode and C=C−H in-plane bending mode as discussed below.

The in-plane C=C−H bending modes coupled with C−C stretching modes appear at around 1200 cm^{-1}. This is the so-called fingerprint region, which is very sensitive to chromophore conformation. In the observed spectrogram, the HOOP mode and C=C−H in-plane bending mode are merged until ~200 fs, followed by the clear separation of the two modes. It elucidates that the rapid tortion along the HOOP coordinate finishes around 200 fs, which is the time when primeRh is reported to appear.[7,32]

The intensities of the HOOP mode and C=C−H in-plane bending mode are also modulated at a period of ~500 fs, reflecting torsional motion around the C_{11}=C_{12} double bond in thermalization from primeRh to bathoRh.

Therefore, when the system crosses CI at 80 fs after excitation, the 200-fs tortional motion along the HOOP coordinate is nearly half finished, and the system is still in the 11-*cis* configuration with partial deformation of the quasi planarity of the plane formed by C_{11}=C_{12}−C_{13} bonds, i.e., the torsional motion around the C_{11}=C_{12} double bond with 500-fs period is (partially) finished with the rotaion angle of about one-sixth (= 80/500) of 180°.

Figure 4c shows two-dimensional Fourier power spectra of the time-resolved difference absorption traces $\Delta A(t)$ over delay times ranging from 800 to 2000 fs. The signals centered at around 60 cm^{-1} confirm that these time-resolved traces are also modulated at a period of ~500 fs, reflecting wavepacket motion at the same period.

In the case of bovine Rh, the transition time from the FC state to CI is reported to be 50 fs,[44] which was estimated as 80 fs for octopus Rh in the present work. For the other transitions with femtosecond and picosecond time constants in bovine Rh, the results are similar to those observed in octopus Rh shown above. Comparing these results with our previous study on transient absorption of bR,[27] we can see that the transition from the FC state to CI proceeds faster in octopus Rh (80 fs) than in bR (~200 fs).

4. CONCLUSIONS

In this work, we have measured time-resolved difference absorption spectra of octopus Rh using a sub-5-fs laser pulse with broadband multichannel detectors. The obtained data matrix has 128 data points in the 528−727-nm region with a 1.56-nm interval and 2100 data points between −100 and 2000 fs with a 1-fs interval. The obtained time-resolved traces were fitted by a double-exponential function using a global fitting method over all probe wavelengths. The time constants of the processes following photoexcitation are comparable between the octopus Rh and bovine Rh results. However, in comparison with the model bR system, the transition time from the FC state to CI in octopus Rh were found to be 80 fs, being about 3 times shorter than in bR, which we measured in transient absorption of bR.[27]

The vibration dynamics of photoisomerization were studied by spectrogram analysis. At delay times shorter than 150 fs, the C=N stretching mode appears and quickly disappears within

150 fs. This observation indicates that the primary event after photoexcitation of the octopus Rh is a deformation of the retinal configuration near the C=N bond in the protonated Schiff base. An observed frequency modulation of the C=C stretching mode at a period of ~500 fs was also observed, reflecting torsional motion around the C_{11}=C_{12} double bond of primeRh before thermalization to bathoRh. This value is similar to the period of 550 fs obtained for wavepacket motion observed in transient absorption measurement of bovine Rh.[40] By contrast, the modulation period for bR was observed to be ~200 fs in transient absorption measurement of bR.[27] On the basis of the frequency change in the C=C stretching mode, the bond length of the C_{11}=C_{12} double bond was found to be modulated on the order of ~10 mÅ. The HOOP and C=C−H modes are merged until 200 fs, therefore the rapid torsion along the HOOP coordinate is thought to be half finished at the delay of 80 fs when the system crosses CI. Their intensities were observed to be modulated at a period of ~500 fs, again affected by the torsional motion around the C_{11}=C_{12} double bond.

AUTHOR INFORMATION

Corresponding Author

*Address: Department of Electrophysics, National Chiao-Tung University, Hsinchu 300, Taiwan. Telephone: 886 3 5712121 ext56197. Fax: 886 3 5725230. E-mail: yabushita@mail.nctu.edu.tw.

ACKNOWLEDGMENTS

This work was supported by the Japan Science and Technology Agency (JST), National Science Council of the Republic of China, Taiwan (NSC 98-2112-M-009-001-MY3, NSC 99-2923-M-009-004-MY3), and a grant from the Ministry of Education, Aiming for Top University (MOE ATU) Program at National Chiao-Tung University (NCTU). This work was also supported in part by a Grant-in-Aid for Scientific Research from the Japan Society for the Promotion of Science (JSPS-GASR-14002003).

REFERENCES

(1) Yoshizawa, T.; Kito, Y. *Nature* **1958**, *182*, 1604−1605.
(2) Yoshizawa, T.; Wald, G. *Nature* **1963**, *197*, 1279−1286.
(3) Buchert, J.; Stefancic, V.; Doukas, A. G.; Alfano, R. R.; Callender, R. H.; Pande, J.; Akita, H.; Balogh-Nair, V.; Nakanishi, K. *Biophys. J.* **1983**, *43*, 279−283.
(4) Horiuchi, S.; Tokunaga, F.; Yoshizawa, T. *Biochim. Biophys. Acta* **1980**, *591*, 445−457.
(5) Eyring, G.; Curry, B.; Mathies, R.; Fransen, R.; Palings, I; Lugtenburg. *J. Biochem.* **1980**, *19*, 2410−2418.
(6) Kandori, H.; Shichida, Y.; Yoshizawa, T. *Biochemistry (Moscow)* **2001**, *66*, 1197−1209.
(7) Kukura, P.; McCamant, D. W.; Yoon, S.; Wandschneider, D. B.; Mathies, R. A. *Science* **2005**, *310*, 1006−1009.
(8) Ohtani, H.; Kobayashi, T.; Tsuda, M.; Ebrey, T. G. *Biophys. J.* **1988**, *53*, 17−24.
(9) Shichida, Y.; Matsuoka, S.; Yoshizawa, T. *Photobiochem. Photobiophys.* **1984**, *7*, 221−228.
(10) Sperling, W. In *Biochemistry and Physiology of Visual Pigments*; Langer, H, Ed.; Springer-Verlag: Heidelberg, 1973; pp 19−28.
(11) Fukada, Y.; Shichida, Y.; Yoshizawa, T.; Ito, M.; Kodama, A.; Tsukida, K. *Biochemistry* **1984**, *23*, 5826−5832.
(12) Mao, B.; Tsuda, M.; Ebrey, T. G.; Akita, H.; Balogh-Nair, V.; Nakanishi, K. *Biophys. J.* **1981**, *35*, 543−546.
(13) Becker, R. S.; Freedman, K. *J. Am. Chem. Soc.* **1985**, *107*, 1477−1485.
(14) Koyama, Y.; Kubo, K.; Komori, M.; Yasuda, H.; Mukai, Y. *Photochem. Photobiol.* **1991**, *54*, 433−443.
(15) Dartnall, H. J. A. *Vision Res.* **1967**, *8*, 339−358.
(16) Kobayashi, T.; Kim, M.; Taiji, M.; Iwasa, T.; Nakagawa, M.; Tsuda, M. *J. Phys. Chem. B* **1998**, *102*, 272−280.
(17) Zhu, L.; Kim, J.; Mathies, R. A. *J. Raman Spectrosc.* **1999**, *30*, 777−783.
(18) Kandori, H.; Sasabe, H.; Nakanishi, K.; Yoshizawa, T.; Mizukami, T.; Shichida, Y. *J. Am. Chem. Soc.* **1996**, *118*, 1002−1005.
(19) Chosrowjan, H.; Mataga, N.; Shibata, Y.; Tachibanaki, S.; Kandori, H.; Shichida, Y.; Okada, T.; Kouyama, T. *J. Am. Chem. Soc.* **1998**, *120*, 9706−9707.
(20) Kandori, H.; Furutani, Y.; Nishimura, S.; Shichida, Y.; Chosrowjan, H.; Shibata, Y.; Mataga, N. *Chem. Phys. Lett.* **2001**, *334*, 271−276.
(21) Schoenlein, R. W.; Peteanu, L. A.; Mathies, R. A.; Shank, C. V. *Science* **1991**, *254*, 412−415.
(22) Kim, J. E.; Mathies, R. A. *J. Phys. Chem. A* **2002**, *106*, 8508−8515.
(23) Shim, S.; Dasgupta, J.; Mathies, R. A. *J. Am. Chem. Soc.* **2009**, *131*, 7592−7597.
(24) Yabushita, A.; Kobayashi, T. *Biophys. J.* **2009**, *96*, 1447−1461.
(25) Pollard, W. T.; Brito Crus, C. H.; Shank, C. V.; Mathies, R. A. *J. Chem. Phys.* **1989**, *90*, 199−208.
(26) Du, M.; Flemming, G. R. *Biophys. Chem.* **1993**, *48*, 101−111.
(27) Kobayashi, T.; Saito, T.; Ohtani, H. *Nature* **2001**, *414*, 531−534.
(28) Baltuska, A.; Kobayashi, T. *Appl. Phys. B: Laser Opt.* **2002**, *75*, 427−443.
(29) Kobayashi, T.; Shirakawa, A.; Matsuzawa, H.; Nakanishi, H. *Chem. Phys. Lett.* **2000**, *321*, 385−397.
(30) Shirakawa, A.; Sakane, I.; Takasaka, M.; Kobayashi, T. *Appl. Phys. Lett.* **1999**, *74*, 2268−2270.
(31) Hozwarth, A. R. *Adv. Photosynth. Respir.* **2004**, *3*, 75−92.
(32) Peteanu, L. A.; Schoenlein, R. W.; Qang, Q.; Mathies, R. A.; Shank, C. V. *Proc. Natl. Acad. Sci. U.S.A.* **1995**, *9*, 11762−11766.
(33) Meier, T.; Mukamel, S. *Phys. Rev. Lett.* **1996**, *77*, 3471−3474.
(34) Rutz, S.; Schreiber, E. *Eur. Phys. J. D* **1998**, *4*, 151−158.
(35) Smith, S. O.; Braiman, M. S.; Myers, A. B.; Pardoen, J. A.; Courtin, J. M. L.; Winkel, C.; Lugtenburg, J.; Mathies, R. A. *J. Am. Chem. Soc.* **1987**, *109*, 3108−3125.
(36) Rothschild, K. J.; Marrero, H. *Proc. Natl. Acad. Sci. U.S.A.* **1982**, *79*, 4045−4049.
(37) Kahan, A.; Nahmias, O.; Friedman, N.; Sheves, M.; Ruhman, S. *J. Am. Chem. Soc.* **2007**, *129*, 537−546.
(38) Pollard, W. T.; Lee, S.-Y.; Mathies, R. A. *J. Chem. Phys.* **1990**, *92*, 4012−4029.
(39) Jean, J. M.; Fleming, G. R. *J. Chem. Phys.* **1995**, *103*, 2092−2101.
(40) Wang, Q.; Schoenlein, R. W.; Peteanu, L. A.; Mathies, R. A.; Shank, C. V. *Science* **1994**, *266*, 422−424.
(41) Gordy, W. *J. Chem. Phys.* **1946**, *14*, 305−320.
(42) Baughman, R. H.; Witt, J. D.; Yee, K. C. *J. Chem. Phys.* **1974**, *60*, 4755−4759.
(43) Dewar, M. J. S. *Hyperconjugation*; Modern Concepts in Chemistry; Ronald Press: New York, 1962; Chapters 3 and 4, pp 48−70.
(44) Kochendoerfer, G. G.; Mathies, R. A. *J. Phys. Chem.* **1996**, *100*, 14526−14532.